*Acta of Bioengineering and Biomechanics*
*Vol. 15, No. 3, 2013*

Original paper
DOI: 10.5277/abb130305

# The comparison of density-elastic modulus equations for the distal ulna at multiple forearm positions: a finite element study

MARK A.C. NEUERT*, REBECCA L. AUSTMAN, CYNTHIA E. DUNNING

Mechanical and Materials Engineering, University of Western Ontario, London, Canada.

The accuracy of an empirically derived density-modulus equation for bone depends upon the loading conditions and anatomic site of bone specimens used for experimentation. A recent study used FE modeling to compare the ability of three density-modulus relationships to predict strain during bending in neutral forearm rotation in the distal ulna; however, due to the inhomogeneous nature of these FE models, the performance of each equation is not necessarily consistent throughout forearm rotation. This issue is addressed in the present study, which compares the performance of these equations in pronation and supination. Strain gauge data were collected at six discreet locations of six ulna specimens loaded in bending at 40° of pronation and supination. Three FE models of each specimen were made, one for each density-modulus relation, and the strain output compared to the experimental data. The equation previously shown to be most accurate in predicting ulnar strain in neutral forearm rotation was also most accurate in pronation and supination. These results identify this one equation as the most appropriate for future FE analysis of the ulna (including adaptive remodeling, and further show that isotropic and inhomogeneous FE bone models may provide consistent results in different planes of bending.

*Key words*: *finite element analysis, density modulus relationship, biomechanics, ulna, implant, experimental validation*

## 1. Introduction

Finite element (FE) models have shown great utility as a compliment to experimental methods in biomechanics [1]–[3] Once validated using *in vitro* methods, a FE model can go on to perform much more insightful analyses, such as predicting changes in bone density over time resulting from stress shielding by prosthetic implants [4]–[8]. These simulations require accurate tissue-level strain estimations as a pre-requisite, and thus rely on accurate assignment of elastic properties.

One approach to defining these properties in bone uses CT data to estimate the spatial distribution of apparent density, which is in turn used to estimate an elastic modulus through an empirical relationship, thus representing the inhomogeneity observed in bone [2], [9], [10]. The accuracy of these relationships depends on the anatomic location of their application [11], [12], as demonstrated by Austman et al., who showed that a density-modulus relation created specifically for the ulna using *in vitro* data more accurately predicted strain values in a FE model of the ulna compared with relations derived from data collected at other anatomic locations.

The ulna-specific equation created by Austman et al. was one step towards a broader goal of developing a bone-remodeling simulation of the distal ulna; however, it was limited in that it only incorporated bending in neutral forearm rotation in its development. The inhomogeneity of bone makes it possible to have different bulk stiffness characteristics in different loading orientations, and a more thorough validation would take this into account. Furthermore, the bone-remodeling analyses in which the relation is to be employed in-

* Corresponding author: Mark Neuert, Mechanical and Materials Engineering, University of Western Ontario, Spencer Engineering Bldg, London, Ontario N6A 5B9, Canada. Tel: 519 661-2111 ext. 8127, fax: 519-661-3020, e-mail: mneuert@uwo.ca

Received: July 22nd, 2012
Accepted for publication: April 15th, 2013

corporate loading in multiple orientations to represent the loading spectrum experienced in activities of daily life [13]–[15].

Thus, the purpose of this study is to extend the validation of the ulna-specific equation developed by Austman et al. [16] to ensure that estimated strain values correlate with those induced experimentally through a range of forearm rotation.

# 2. Materials and methods

## 2.1. Experimental testing

Six fresh-frozen right ulnae (mean age = 66 ± 8 years; 5 male, 1 female) were cleaned of all soft tissue, thawed, and fixed proximally into a custom jig. Six pairs of uniaxial strain gauges were applied to medial and lateral surfaces of the bone (Fig. 1), and integrated into a Wheatstone half-bridge configuration. The jig was then placed in a materials testing machine (Instron 8872, Canton, MA, USA). Strain data were recorded while a 20 N load was applied to the distal articular surface of the ulnar head. The load application point was varied by rotating the jig relative to the actuator in 40° of pronation or supination (Fig. 1).

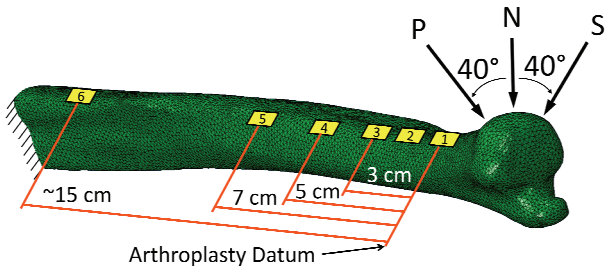


Fig. 1. (A) Experimental setup and (B) strain gauge locations and loading directions (only lateral gauges shown; P = pronation, N = neutral, S = supination). Strain gauge 1 corresponds to the interface between diaphysis and epiphysis (distal ulnar head), corresponding to the resection plane used in distal ulnar arthroplasty

## 2.2. Finite element modelling

Each ulna was scanned using a micro-CT scanner with isotropic 152 µm voxel spacing (eXplore Ultra, GE Healthcare, London, Canada). Surface geometry was extracted using Mimics (Materialise, Leuven, Belgium) and imported into the FE software Abaqus (Simulia, Providence, RI, USA) where a 3-D model was created, and subsequently meshed using second-order tetrahedral elements of characteristic length 0.75 mm.

A program developed in-house used CT data to assign a density value to each element of the model meshes. The program worked by first assigning each voxel a density value based on a comparison of its Hounsfield value with that of a calibration phantom of a known density included in the scan (to correct for edge effects, any voxel with a volume only partially inside the bone's CT-based outer boundary were excluded.) Then an elastic modulus was calculated for each voxel using one of three density-modulus equations, chosen on their proven ability to predict strain values in the ulna [17].

$$E = 8346\rho_{\text{app}}^{1.5} \text{ (Austman et al. [16])}, \quad (1)$$

$$E = 2875\rho_{\text{app}}^{3} \text{ (Carter and Hayes [19])}, \quad (2)$$

$$E = 8920\rho_{\text{app}}^{1.83} \text{ (Morgan et al. [12])}. \quad (3)$$

An elastic modulus was then assigned to each mesh element by averaging the modulus values calculated for each voxel contained within that element's volume.

Modeling the experimental set-up, a 20 N force was applied to the articular surface of each model at 40° of pronation and supination (Fig. 1).

In summary, FE models of six ulna specimens were loaded in two orientations using three density-modulus relations, totaling 36 finite element models. The mesh elements corresponding to the strain gauge locations were identified for all models, and the surface strain predicted at these locations were compared to their corresponding experimental readings.

## 2.3. Statistical analysis

Two-way repeated measures (RM) ANOVAs with main factors of strain gauge location (site 1–6) and density modulus equation were used to compare model and experimental strain output values across all gauge locations, with Student–Newman–Keuls tests for post-hoc analyses ($\alpha$ = 0.05). Root-mean-squared errors (RMSE) across all gauge locations were calculated for each specimen as a measure of error magnitude. Intraclass correlation coefficients (ICCs) were calculated to examine the correlation between experimental and predicted strain. In addition, Bland–Altman plots (a more appropriate method for assessing the degree of agreement between two measurement

methods than a simple correlation [18]) were constructed to detect any biases or systemic errors.

# 3. Results

The two-way RM ANOVA showed an interaction between gauge location and density-modulus equation used ( $p < 0.05$) in both pronation and supination. Therefore, separate one-way RM ANOVAs were performed comparing strain results at each gauge location (Table 1).

At all gauge locations in both pronation and supination, Equation (1) was not found to significantly differ from the experimental strain values ( $p > 0.05$). Equation (3) performed well at the distal gauges with $p > 0.05$ at gauge 1 in pronation and gauges 1 and 2 in supination. Equation (2) performed well at gauge 4 in pronation and gauges 4 and 5 in supination ( $p > 0.05$).

The RMSE of strain predicted by each equation for each individual specimen is presented in Table 2. In pronation, Equation (1) displayed the lowest RMSE in five of the six specimens, with the sixth specimen being best represented by Equation (2). In supination, Equation (1) had the lowest RMSE values in three specimens, Equation (3) in two specimens, and Equation (2) in one specimen. Averaged across all specimens, Equation (1) had the lowest RMSE in both pronation (26.6 με) and in supination (34.1 με).

Bland–Altman plots between experimental and predicted strain were constructed for each equation

Table 1. P-values obtained from the modeled and experimental strain values at each gauge location for pronation and supination. Strain values not significantly different from experimental measurements ( $p > 0.05$) have been bolded

| | | Supination | | | Pronation | | |
|---|---|---|---|---|---|---|---|
| | Gauge location | Eq. (1) | Eq. (2) | Eq. (3) | Eq. (1) | Eq. (2) | Eq. (3) |
| Distal | 1 | **0.42** | <0.01 | **0.49** | **0.79** | 0.01 | **0.92** |
| | 2 | **0.49** | 0.02 | **0.06** | **0.37** | 0.01 | 0.02 |
| | 3 | **0.44** | 0.02 | <0.01 | **0.74** | 0.01 | <0.01 |
| | 4 | **0.88** | **0.17** | <0.01 | **0.22** | **0.22** | <0.01 |
| | 5 | **0.83** | **0.17** | <0.01 | **0.36** | 0.03 | <0.01 |
| Proximal | 6 | **0.84** | 0.05 | <0.01 | **0.86** | <0.01 | <0.01 |

Table 2. RMSE for strain values predicted using each equation, averaged over all six gauge locations for pronation and supination. The overall RMSE for each equation is given at bottom. The range of strain values for all gauge locations recorded for each specimen in a given orientation is given at right, in order to put into perspective the relative magnitude of RMSE compared to absolute strain values

| | Supination (με) | | | | Pronation (με) | | | |
|---|---|---|---|---|---|---|---|---|
| | RMSE | | | Range | RMSE | | | Range |
| Specimen | Eq. (1) | Eq. (2) | Eq. (3) | | Eq. (1) | Eq. (2) | Eq. (3) | |
| 1 | 21.6 | 37.8 | **17.2** | 48–145 | **25.5** | 32.5 | 60.3 | 119–231 |
| 2 | **25.4** | 88.8 | 41.2 | 104–177 | **37.5** | 141.2 | 38.5 | 145–301 |
| 3 | **23.6** | 67.5 | 30.2 | 85–317 | **20.8** | 48.4 | 36.9 | 110–247 |
| 4 | **16.5** | 39.0 | 25.4 | 33–176 | 27.7 | **22.5** | 69.9 | 111–277 |
| 5 | 64.4 | **50.9** | 105.3 | 85–269 | **20.3** | 32.1 | 72.9 | 108–294 |
| 6 | 29.9 | 43.6 | **9.6** | 37–170 | **23.8** | 51.1 | 28.5 | 88–249 |
| | | | | | | | | |
| Overall | **34.1** | 57.6 | 49.5 | | **26.6** | 67.7 | 54.0 | |

Table 3. Mean difference and limits of agreement values for the Bland–Altman plots for each equation in pronation and supination. Limits of Agreement correspond to ±1.96 standard deviations

| | Supination | | | Pronation | | |
|---|---|---|---|---|---|---|
| Equation | Eq. (1) | Eq. (2) | Eq. (3) | Eq. (1) | Eq. (2) | Eq. (3) |
| Mean difference | 5.8 με | 34.5 με | –29.1 με | 1.0 με | 39.8 με | –41.7 με |
| Limits of agreement | ±34.1 με | ±46.7 με | ±40.7 με | ±26.9 με | ±55.5 με | ±34.8 με |

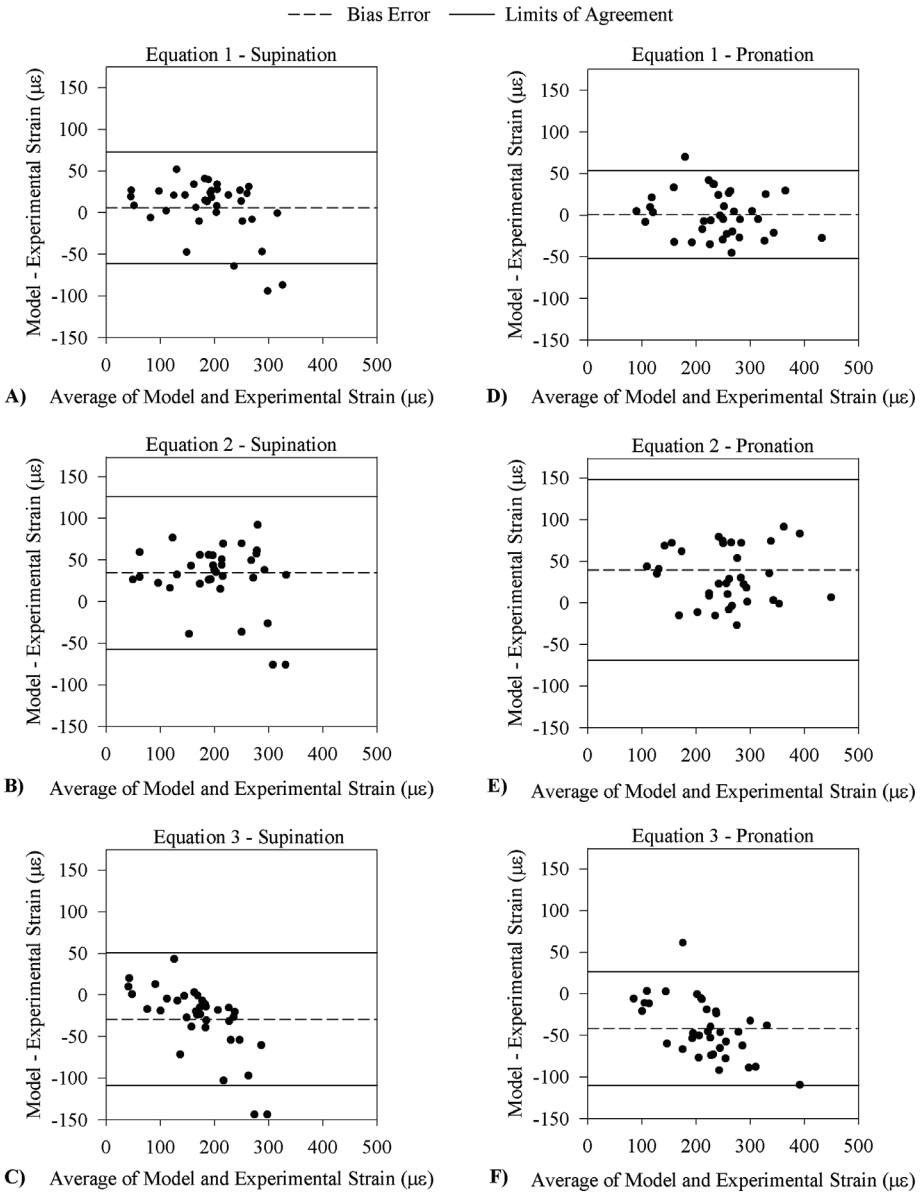


Fig. 2. Bland–Altman plots for each equation in supination (A–C) and pronation (D–F)

Table 4. Intraclass Correlation Coefficients between experimental strain values and those calculated for each equation in pronation and supination

| | Supination | | | Pronation | | |
|---|---|---|---|---|---|---|
| Equation | Eq. (1) | Eq. (2) | Eq. (3) | Eq. (1) | Eq. (2) | Eq. (3) |
| ICC | **0.90** | 0.75 | 0.77 | **0.94** | 0.69 | 0.75 |
| Lower bound | 0.81 | 0.36 | 0.41 | 0.89 | 0.29 | 0.04 |
| Upper bound | 0.95 | 0.89 | 0.90 | 0.97 | 0.85 | 0.92 |

(Fig. 2). The mean difference and limits of agreement for each plot are displayed in Table 3. In both pronation and supination, Equation (2) tended to overestimate, and Equation (3) underestimate, experimental strain values. Equation (1) displayed the smallest bias error, and the tightest limits of agreement, with a slight tendency to overestimate strain in supination only.

Regarding ICC values (Table 4), Equation (1) calculated strains that correlated best with experimental values and had the narrowest 95% confidence interval in pronation and supination.

# 4. Discussion

Past studies have shown that bending load orientation influences the accuracy of isotropic, inhomogeneous FE bone models created using a density-modulus equation. One such equation developed from *in vitro* ulnar strain data by Austman et al. [16] has proven more accurate than those developed using data from other anatomic locations (Carter and Hayes [19] and Morgan et al. [12]) in its ability to predict ulnar strain; however, these tests were conducted in neutral forearm rotation only. The present study expanded upon this previous work by extending the validation procedure to include 40° of pronation and supination, thus representing the ulna's range of motion.

According to the RM ANOVAs, only the strain results acquired using Equation (1) (Austman et al. [16]) did not significantly differ from experimental values at any gauge location. Furthermore, Equation (1) displayed the lowest overall RMSE and highest ICC values with the narrowest 95% confidence interval. The Bland–Altman plots showed that Equation (1) had the smallest bias error and limits of agreement in pronation and supination.

These results compare well with those of Austman et al. [16], who reported RMSE, ICC values, mean differences and limits of agreement of 29.21 με, 0.94 (lower bound 0.80, upper bound 0.97), 19.0 με and ±27.7 με, respectively, using the same experimental setup in neutral forearm rotation. Furthermore, strain values acquired in the present study follow trends similar as in Austman et al. [16]; specifically that Equation (2) (Carter and Hayes [19]) tended to overestimate, and Equation (3) (Morgan et al. [12]), underestimate, strain values; and furthermore, that Equation (3) showed smaller error values at gauges placed closest to the epiphysis (distally at gauges 1 and 2), while Equation (2) performed best at gauges completely in the diaphysis (gauges 5 and 6). This consistency for all three equations suggests that strain output of an isotropic, inhomogeneous model undergoing longitudinal bending is independent of bending orientation for the ulna.

A major limitation of this study is the use of uniaxial strain gauges, as strain gauge rosettes would have allowed for comparisons of principal shear strain values and directions; however, to use rosettes at six locations would require recording of 18 channels, which could not be done simultaneously using the available data acquisition capabilities. The decision to use uniaxial gauges was based on a desire to simultaneously collect strain at multiple locations longitudinally along the ulna before and after implantation of stemmed prosthetic, as part of an overarching investigation of load transfer in the ulna.

In order to mitigate the inability to measure shear stresses, loading was limited to longitudinal bending, producing predominantly normal bending stresses. This was justified by the fact that the bending loading condition reflects *in vitro* observations of physiological ulnar loading [20].

Another limitation of the study is the use of an isotropic material model of bone, which exhibits orthotropic material properties [21]–[23]. While the assumption isotropy material is not ideal, CT data only provides scalar information, and the determination of principal material directions must be inferred (e.g., orientation of material directions with anatomical landmarks). In addition, the assumption of an inhomogeneous, isotropic model has shown to be comparable to anisotropic models of long bone in the absence of shear stresses [24], [25] particularly in the diaphysis [26], [27], and as mentioned, the predominant loading case of the ulna is in bending with negligible torsion [20].

Furthermore, the application for which the equation is being used needs to be considered. Despite the limits of this study's experimental and numerical components, the clinical value of this work is significant. Inhomogeneous, isotropic models of bone, such as the one presented here, have been successfully implemented in strain adaptive models of human bone [13], [28]–[32]. A sample of the knowledge gleaned from such studies include the assessment of the potential benefits of new procedures such as joint resurfacing versus replacement [14], and identification of the relative importance of various muscle and contact forces within a joint system [33]. The results of the present study represent an important step towards the authors' long-term goal of developing a strain-adaptive model of the ulna to evaluate the long term affects of arthroplasty in the distal radio-ulnar joint (DRUJ), a subject which represents a significant lack of knowledge in the literature with regards to biomechanics in general and bone remodeling in particular.

In conclusion, the data gathered in the present study identify the density-modulus equation developed by Austman et al. [16] as the best current model of the elastic properties of the ulna for subject-specific finite element models, accurately predicting strain through a range of motion in 40° of pronation and supination.

## References


[1] KERNER J., HUISKES R., van LENTHE G.H., WEINANS H., van RIETBERGEN B., ENGH C.A., AMIS A.A., *Correlation between pre-operative periprosthetic bone density and post-operative bone loss in THA can be explained by strain-adaptive remodelling*, Journal of Biomechanics, 1999, Vol. 32, 695–703.

[2] SCHILEO E., TADDEI T., MALANDRINO A., CRISTOFOLINI L., VICECONTI M., *Subject-specific finite element models can accurately predict strain levels in long bones*, Journal of Biomechanics, 2007, Vol. 40, 2982–2989.

[3] TADDEI F., VICECONTI M., MANFRINI M., TONI A., *Mechanical strength of a femoral reconstruction in paediatric oncology: A finite element study*. Proceedings of the Institution of Mechanical Engineers, Part H: Journal of Engineering in Medicine, 2003, Vol. 217, 111–119.

[4] GARCÍA J., DOBLARÉ M., CEGOÑINO J., *Bone remodelling simulation: a tool for implant design*, Computational Materials Science, 2002, Vol. 25, 100–114.

[5] HUISKES R., WEINANS H., DALSTRA M., *Adaptive bone remodeling and biomechanical design considerations for noncemented total hip arthroplasty*, Orthopedics, 1989, Vol. 12, 1255–1267.

[6] PÉREZ M.A., FORNELLS P., DOBLARÉ M., GARCÍA-AZNAR J.M., *Comparative analysis of bone remodelling models with respect to computerised tomography-based finite element models of bone*, Computer Methods in Biomechanics and Biomedical Engineering, 2010, Vol. 13, 71–80.

[7] WEINANS H., HUISKES R., GROOTENBOER H.J., *Effects of material properties of femoral hip components on bone remodeling*, Journal of Orthopaedic Research, 1992, Vol. 10, 845–853.

[8] WEINANS H., HUISKES R., van RIETBERGEN B., SUMNER D.R., TURNER T.M., GALANTE J.O., *Adaptive bone remodeling around bonded noncemented total hip arthroplasty: A comparison between animal experiments and computer simulation*, Journal of Orthopaedic Research, 1993, Vol. 1, 500–513.

[9] LEUNG A.S.O., GORDON L.M., SKRINSKAS T., SZWEDOWSKI T., WHYNE C.M., *Effects of bone density alterations on strain patterns in the pelvis: Application of a finite element model*, Proceedings of the Institution of Mechanical Engineers, Part H: Journal of Engineering in Medicine, 2009, Vol. 223, 965–979.

[10] TADDEI F., CRISTOFOLINI L., MARTELLI S., GILL H.S., VICECONTI M., *Subject-specific finite element models of long bones: An in vitro evaluation of the overall accuracy*, Journal of Biomechanics, 2006, Vol. 39, 2457–2467.

[11] KALOUCHE I., CRÉPIN J., ABDELMOUMEN S., MITTON D., GUILLOT G., GAGEY O., *Mechanical properties of glenoid cancellous bone*, Clinical Biomechanics, 2010, Vol. 25, 292–298.

[12] MORGAN E.F., BAYRAKTAR H.H., KEAVENY T.M., *Trabecular bone modulus-density relationships depend on anatomic site*, Journal of Biomechanics, 2003, Vol. 36, 897–904.

[13] BEAUPRÉ G.S., ORR T.E., CARTER D.R., *An approach for time-dependent bone modeling and remodeling – application: A preliminary remodeling simulation*, Journal of Orthopaedic Research, 1990, Vol. 8, 662-670.

[14] DABIRRAHMANI D., HOGG M., KOHAN L., GILLIES M., *Primary and long-term stability of a short-stem hip implant*, Proceedings of the Institution of Mechanical Engineers, Part H: Journal of Engineering in Medicine, 2010, Vol. 224, 1109–1119.

[15] SHARMA G.B., DEBSKI R.E., McMAHON P.J., ROBERTSON D.D., *Adaptive glenoid bone remodeling simulation*, Journal of Biomechanics, 2009, Vol. 42, 1460–1468.

[16] AUSTMAN R.L., MILNER J.S., HOLDSWORTH D.W., DUNNING C.E., *Development of a customized density-modulus relationship for use in subject-specific finite element models of the ulna*, Proceedings of the Institution of Mechanical Engineers, Part H: Journal of Engineering in Medicine, 2009, Vol. 223, 787–794.

[17] AUSTMAN R.L., MILNER J.S., HOLDSWORTH D.W., DUNNING C.E., *The effect of the density-modulus relationship selected to apply material properties in a finite element model of long bone*, Journal of Biomechanics, 2008, Vol. 41, 3171–3176.

[18] BLAND J.M., ALTMAN D.G., *Statistical methods for assessing agreement between two methods of clinical measurement*, Lancet, 1986, Vol. 1, 307–310.

[19] CARTER D.R., HAYES W.C., *The compressive behavior of bone as a two-phase porous structure*, Journal of Bone and Joint Surgery - Series A, 1977, Vol. 59, 954–962.

[20] GORDON K.D., KEDGLEY A.E., FERREIRA L.M., KING G.J.W., JOHNSON J.A., *Effect of simulated muscle activity on distal radioulnar joint loading in vitro*, Journal of Orthopaedic Research 2006, Vol. 24, 1395–1404.

[21] DEMPSTER W.T., LIDDICOAT R.T., *Compact bone as a non-isotropic material*, The American Journal of Anatomy, 1952, Vol. 91, 331–362.

[22] GOULET R.W., GOLDSTEIN S.A., CIARELLI M.J., KUHN J.L., BROWN M.B., FELDKAMP L.A., *The relationship between the structural and orthogonal compressive properties of trabecular bone*, Journal of Biomechanics, 1994, Vol. 27, 375–389.

[23] MARTENS M., van AUDEKERCKE R., DELPORT P., *The mechanical characteristics of cancellous bone at the upper femoral region*, Journal of Biomechanics, 1983, Vol. 16, 971–983.

[24] BARKER D.S., NETHERWAY D.J., KRISHNAN J., HEARN T.C., *Validation of a finite element model of the human metacarpal*, Medical Engineering and Physics, 2005, Vol. 27, 103–113.

[25] YANG H., MA X., GUO T., *Some factors that affect the comparison between isotropic and orthotropic inhomogeneous finite element material models of femur*, Medical Engineering and Physics, 2010, Vol. 32, 553–560.

[26] BACA V., HORAK Z., MIKULENKA P., DZUPA V., *Comparison of an inhomogeneous orthotropic and isotropic material models used for FE analyses*, Medical Engineering and Physics, 2008, Vol. 30, 924–930.

[27] PENG L., BAI J., ZENG X., ZHOU Y., *Comparison of isotropic and orthotropic material property assignments on femoral finite element models under two loading conditions*, Medical Engineering and Physics, 2006, Vol. 28, 227–233.

[28] GUPTA S., NEW A.M.R., TAYLOR T., *Bone remodelling inside a cemented resurfaced femoral head*, Clinical Biomechanics, 2006, Vol. 21, 594–602.

[29] HUISKES R., WEINANS H., GROOTENBOER H.J., DALSTRA M., FUDALA B., SLOOFF T.J., *Adaptive bone-remodeling theory applied to prosthetic-design analysis*, Journal of Biomechanics, 1987, Vol. 20, 1135–1150.

[30] SHARMA G.B., DEBSKI R.E., McMAHON P.J., ROBERTSON D.D., *Effect of glenoid prosthesis design on glenoid bone remodeling: Adaptive finite element based simulation*, Journal of Biomechanics, 2010, Vol. 43, 1653–1659.

[31] STÜLPNER M.A., REDDY B.D., STARKE G.R., SPIRAKIS A., *A three-dimensional finite analysis of adaptive remodelling in the proximal femur*, Journal of Biomechanics, 1997, Vol. 30, 1063–1066.

[32] TURNER A.W.L., GILLIES R.M., SEKEL R., MORRIS P., BRUCE W., WALSH W.R., *Computational bone remodelling simulations and comparisons with DEXA results*, Journal of Orthopaedic Research, 2005, Vol. 23, 705–712.

[33] BITSAKOS C., KERNER J., FISHER I., AMIS A.A., *The effect of muscle loading on the simulation of bone remodelling in the proximal femur*, Journal of Biomechanics, 2005, Vol. 38, 133–139.